On the study of wire cutting of starch gels

C. Gamonpilas[1,2], M. Charalambides[1], J.G. Williams[1], P.J. Dooling[3], S.R. Gibbon[3]

[1]Imperial College London, Mechanical Engineering Department, London SW7 2AZ, UK, [2]Current address: National Metal and Materials Technology Center (MTEC), Pathumthani, Thailand, [3]Akzo Nobel Research Development and Innovation, Wilton Applied Research Group, UK.

ABSTRACT

Wire cutting experiments were performed to study the fracture behaviour of starch gels. The results showed that the fracture toughness increases with cutting speed. This is consistent with the results obtained from the independent conventional fracture mechanics test. Finite element simulations of wire cutting process were also performed. A non-linear elastic constitutive relationship was used to model the starch gels and frictionless condition was assumed at the wire-starch gel contact interface. A failure criterion based on critical fracture strain was assumed. Predictions of the steady-state cutting force at various wire diameters and cutting speeds were found to be in good agreement with the wire cutting data.

1 INTRODUCTION

The study of the fracture properties is very important in food technology and in the production of consumer products. Industrial processes involving fracture or separation of the material, e.g. cutting, slicing etc, are very common. Fracture of food also occurs during mastication. Understanding and optimising such processes requires the knowledge of the material and fracture behaviour, i.e. establishing suitable failure criteria, which can be used to predict the cutting force. One test which has been employed for measuring the fracture properties of foods is wire cutting. Typically, a wire is pushed into the material until a steady state cutting force is achieved. A typical force-displacement trace for a wire cutting test can be found in Fig. 1, demonstrating the two phases of the process. In the first phase, the wire indents into the material. At some point during the indentation, the material starts to fracture and a steady state cutting phase proceeds.

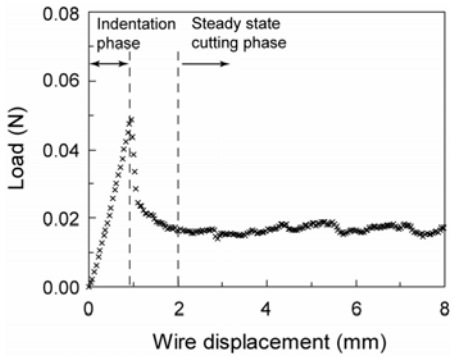

FIG. 1: Example of force-displacement relationship in the wire cutting test (2-34 (10%) gel, wire diameter of 0.25 mm and cutting speed of 5 mm/min).

In the wire cutting process, fracture, large deformation and surface friction occur simultaneously [1,2]. It has been stated by [3] that the force F required for cutting is proportional to the wire diameter (d) and that there is a constant component arising from G_c, the fracture toughness. The proportionality factor with the diameter was then determined from the deformation energy and the friction. A linear equation between the cutting force and wire diameter was developed by [1] and has the form of;

$$\frac{F}{b} = G_c + (1+\mu)\sigma_y d \qquad \text{(Eq. 1)}$$

where b is the width of the sample, σ_y is the characteristic stress and μ is the coefficient of friction.

Under uniaxial compression loading, starch gels exhibit rate independent stress-strain behaviour but show rate-dependent fracture behaviour i.e. stress-strain curves at three loading strain rates are similar but fracture strain and fracture stress increase with increasing strain rate [4]. This is rather unusual behaviour. Therefore, the objective of this work is to investigate the fracture behaviour of starch gels using wire cutting experiments. Independent conventional fracture mechanics tests using single-edge notched beams (SENB) were also performed in order to validate the results obtained from the wire cutting tests. In addition, numerical models were utilised to predict the steady state cutting force.

2 EXPERIMENTS

Two starch gels, e.g. 2-34 (modified sago starch) and 2-12 (modified maize starch), were investigated. Samples were prepared as described in [4]. Two fracture experiments were performed using the Instron 5543 machine at 21^{o}C and 50% relative humidity and these are described as follows;

2.1 Wire cutting

Wire cutting tests, shown in Fig. 2(a), were performed at three cutting speeds (V) of 0.5, 5 and 50 mm/min. Various powder concentrations were studied i.e. 15 and 20% for 2-34 and 20% for 2-12. Steel wire diameters, d, of 0.1, 0.25, 0.4 and 0.5 mm were used. The specimens for the wire cutting tests were rectangular blocks of length 30 mm, width 20 mm and height 20 mm. A 10N load cell was used as the cutting load on gels was generally small.

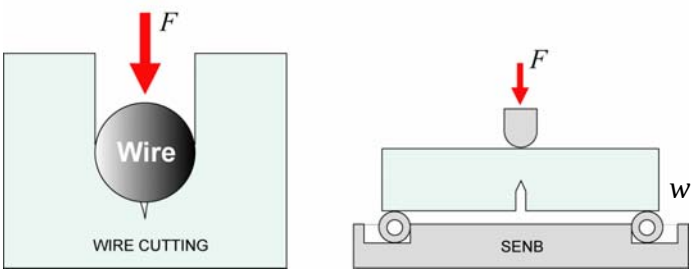

(a) (b)

FIG. 2: Illustrations of fracture tests (a) wire cutting and (b) SENB.

2.2 Single-edge notched beam (SENB)

SENB tests, shown in Fig. 2(b), were conducted according to the ESIS protocol described in [5]. Specimens were rectangular blocks of length, L = 90 mm, width, w = 20 mm (see Fig. 2(b)) and breadth, b = 10 mm. A length span of 80 mm and a notch depth of approximately 2 mm were used in these tests. The specimen notch size did not follow the ESIS protocol. This modification was necessary to prevent immediate fracture due to the sample's own weight. Similar to the wire cutting experiments, tests were performed at three constant crosshead speeds of 0.5, 5 and 50 mm/min. Only two materials, e.g. 2-34 (15%) and 2-34 (20%), were tested as others were too compliant and soft for this type of test.

3 NUMERICAL SIMULATION OF WIRE CUTTING

Finite element simulations were performed to study the wire cutting process and to predict the steady state cutting force at various wire diameters. The simulations were performed using the commercial finite element code ABAQUS [6]. The geometry of the FE model is based on the actual specimen sizes and is shown schematically in Fig. 3(a). The bulk material was modelled using four noded, plane strain solid elements with the material parameters taken from those calibrated from the monotonic compression data. A hyperelastic model based on Ogden was chosen as the constitutive model [4]. The wires were defined as rigid surfaces and were prescribed to move along y-direction. The bottom surface of the models was constrained in the y-direction but was allowed to move freely in the x-direction. A finer mesh was used along the cutting path to improve the accuracy and convergence of the solution (Fig. 3(b)).

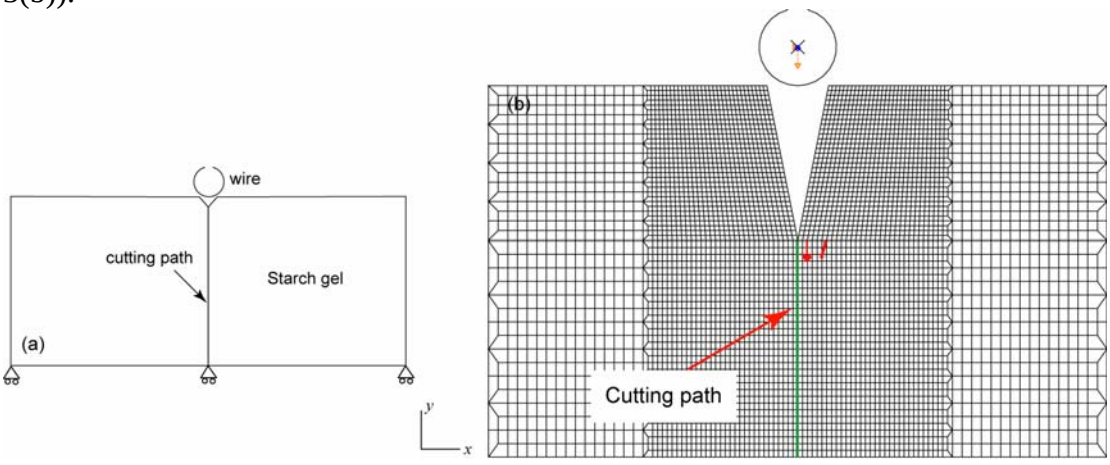

FIG. 3: (a) Finite element geometry for wire cutting model and (b) typical mesh used in simulation.

The steady state cutting phase was simulated using a node-release technique. The nodes along the cutting path are released, and so the crack allowed to propagate, when the maximum principal strain at a distance l ahead of the wire attains a critical value (Fig. 3(b)). The distance l was obtained from the FE simulation of the indentation phase, i.e. it was taken to be equal to the distance from the initial crack tip

to the point where the principal strain attained its maximum value. The critical distance l increased with wire diameter. The critical strain value as a function of cutting speed was first determined such that the cutting force predictions matched the experimental data for the wire diameter of 0.25 mm. The nodal release technique was implemented through the MPC subroutine in ABAQUS [6]. It was assumed in the FE analysis that the crack grows in the plane of cutting, i.e. along the symmetry plane. A frictionless condition was assumed at the interface between the wire and material.

4 RESULTS AND DISCUSSION

Fig. 4 shows the force-displacement curves of wire cutting tests on 2-34 (15%) for wire diameters of 0.1, 0.25, 0.4 and 0.5 mm and cutting speeds of 0.5, 5 and 50 mm/min. For each wire diameter, the indentation part of the curves are found to be similar for all cutting speeds, suggesting that mechanical properties are rate independent. However, it was observed that the steady state force values increase with cutting speeds for all wire diameters. As a result, it can be concluded that the fracture behavior is rate dependent. This agrees with the compression results that compressive failure strain was a function of strain rate [4]. It was also shown that larger cutting forces were obtained with higher cutting speeds. There is also a notable fluctuation, which seems to increase with the diameter of the cutting wire. This large scatter at larger diameters was also observed in the wire cutting study on cheese and it was attributed to secondary micro-cracking [2].

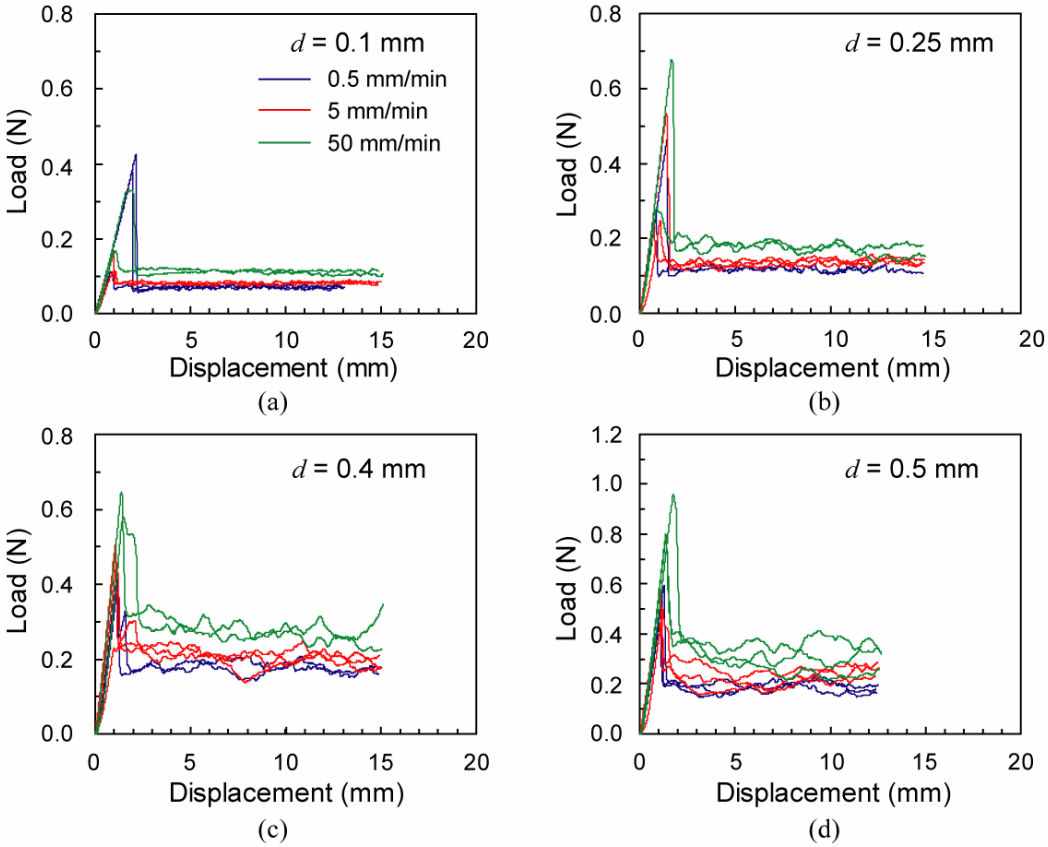

FIG. 4: Experimental wire cutting data of 2-34 (15%) at different cutting speeds and wire diameters of (a) 0.1, (b) 0.25, (c) 0.4 and (d) 0.5 mm.

Further analysis on fracture energy was done by plotting the normalised values of the average values of steady state cutting force (*F/b*) against wire diameter. This is shown in Figs. 5(a)-(c) for 2-34 (15%), 2-34 (20%) and 2-12 (20%), respectively. It can be seen that the steady state cutting force increases almost linearly with wire diameter for all materials. The relationship was fitted with Eq. (1) to obtain the fracture toughness, characteristic stress and friction coefficient. The fracture toughness was assumed to be constant for different wire diameters and was extrapolated to the theoretical zero wire diameter. The fits are generally good with R^2 greater than 0.95 for all cases. The values of G_c were found be rate dependent and increase with increasing cutting speeds. In addition, the values are relatively small as expected and are found to be between 1.9-3.1 J/m^2 for the 2-34 gel and 0.3-1.2 J/m^2 for the 2-12 gel.

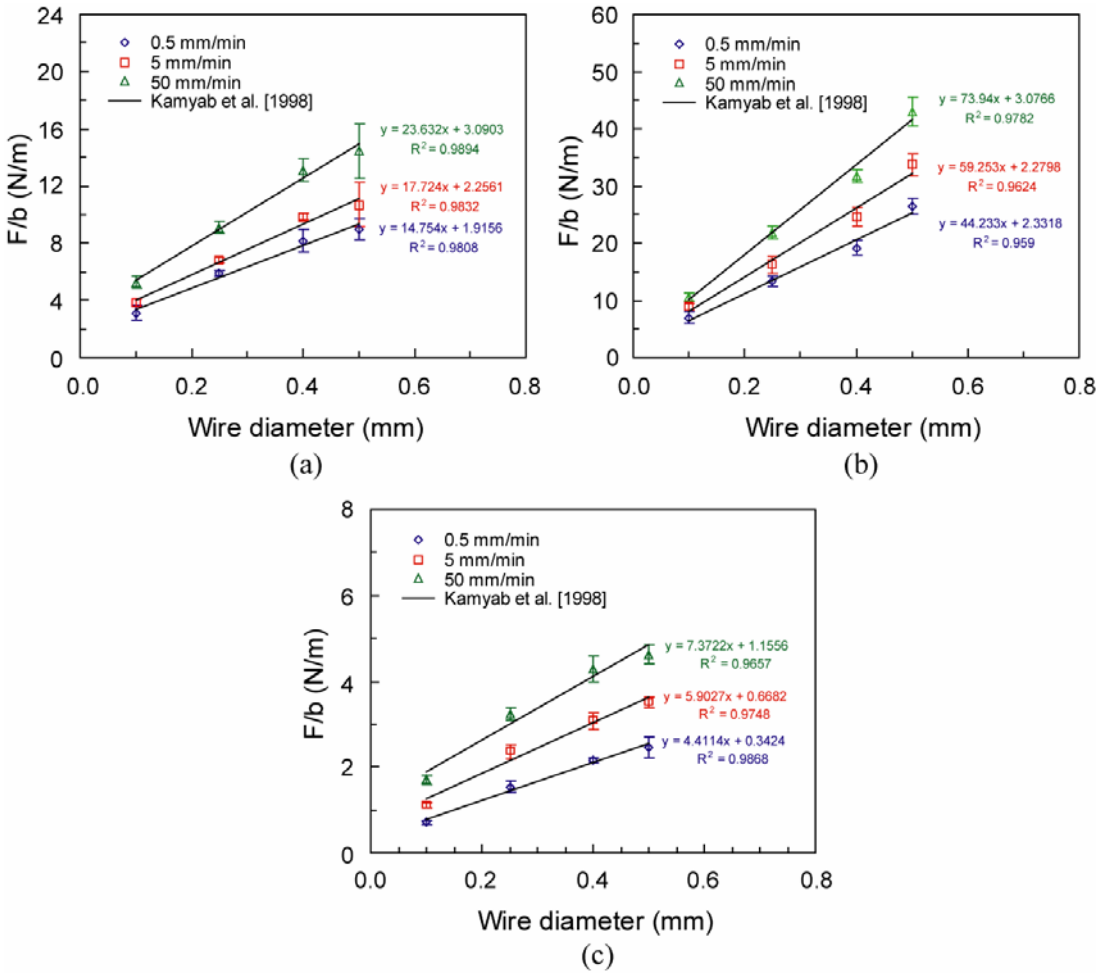

FIG. 5: Experimental wire cutting data at different cutting speeds for (a) 2-34(15%), (b) 2-34(20%) and (c) 2-12(20%).

The extrapolation procedure shown in Fig. 5 pose the further question as what strain rates the extrapolated G_c values correspond to. Eq. (1) was derived based on the assumption of rate-independent, elastic-perfectly plastic behaviour so the strain rate

effect was not taken into account. For the rate dependent case, the following relationships were assumed;

$$\sigma_y = \sigma_0 \left(\frac{\dot{\varepsilon}}{\dot{\varepsilon}_0} \right)^m \quad \text{and} \quad G_c = G_0 \left(\frac{\dot{\varepsilon}}{\dot{\varepsilon}_0} \right)^n \qquad \text{(Eq. 2)}$$

where $\dot{\varepsilon}_0$ has the value of 1/min and is included so that the equations are dimensionally correct. The term G_0 is the fracture toughness at $\dot{\varepsilon}_0 = 1/\min$, and σ_0 is a characteristic stress at $\dot{\varepsilon}_0 = 1/\min$. An approximate relationship between $\dot{\varepsilon}$, d and V was assumed in the form of $\dot{\varepsilon} = \frac{KV}{d + C}$ where K and C are constants. The constants K and C were calibrated by fitting the expression with the strain rate calculated from the FE simulation of the indentation phase for each wire diameter. The strain rate at each cutting speed was calculated through the chain rule, $\frac{d\varepsilon}{dt} = \frac{d\varepsilon}{d\delta} \times \frac{d\delta}{dt}$ where δ is the displacement and $\frac{d\delta}{dt}$ is the cutting speed. The expression $\frac{\partial \varepsilon}{\partial \delta}$, which describes how the maximum tensile strain changes with the wire displacement, was obtained from the FE simulation. Fig. 6 shows the typical contour plot of tensile strain, ε_{xx}, in the region around the cutting wire.

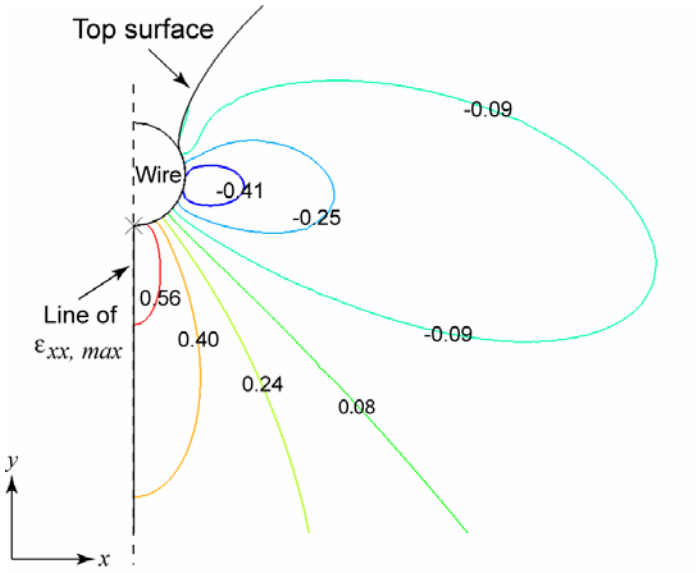

FIG. 6: Typical contour plot of the strain in the *x*-direction for the wire cutting simulation on 2-34 (15%) gel with *d* = 0.4 mm.

By assuming σ_y to be the fracture stress of the material obtained from compression tests, it was found that the value of *m* is similar to *n*, as shown in Fig. 7. Hence, Eq. (1) may now be written as,

$$\frac{F}{b}\left(\frac{\dot{\varepsilon}_0(d+C)}{KV}\right)^m = G_0 + (1+\mu)\sigma_0 d \qquad \text{(Eq. 3)}$$

where $m \approx n = 0.10$.

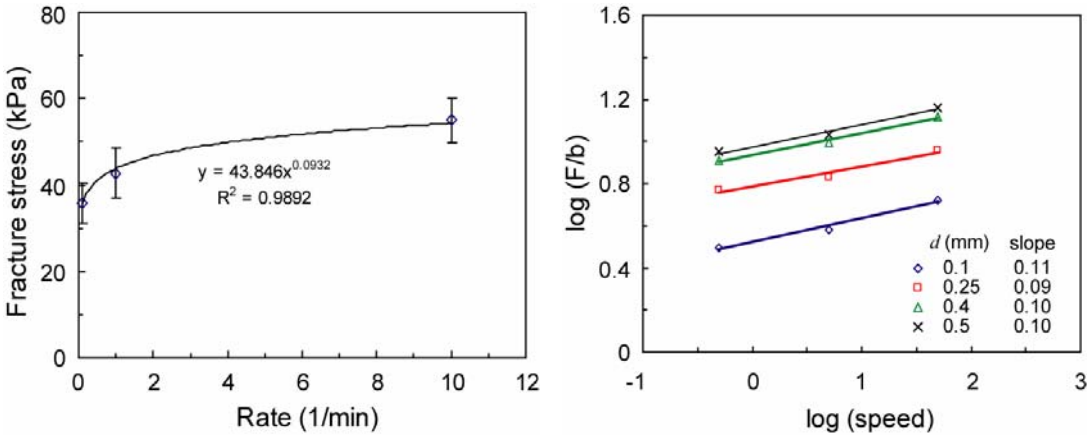

(a) (b)

FIG. 7: Relationship between (a) fracture stress and strain rate and (b) cutting energies and speed of 2-34(15%).

Fig. 8 shows the cutting data in Fig. 5 replotted according to Eq. (3). The agreement between the corrected F/b values for different test speeds shows that the rate dependent effects are approximated well by Eq. (3). By fitting the data points with the linear relationship, the values of G_0 were found to be 0.44, 1.96 and 2.87 J/m^2 for 2-12 (20%), 2-34 (15%) and 2-34 (20%), respectively. These also agree with the simpler analysis results obtained from Eq. (1). For comparison purposes, the values of G_0 for mild Cheddar and Gruyere are 6.0 J/m^2 and 3.7 J/m^2, respectively [2].

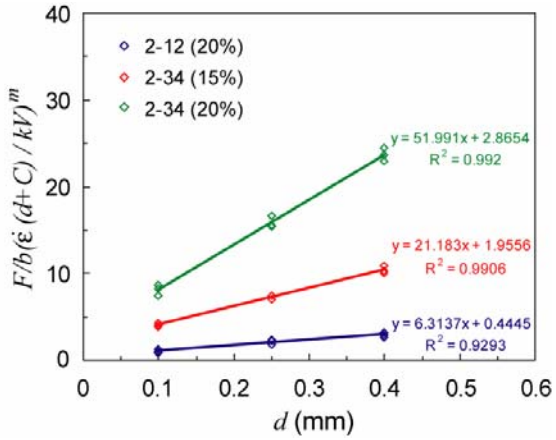

FIG. 8: Experimental wire cutting data plotted according to Eq. (3).

Figs. 9(a) and 9(b) show load-displacement curves at three loading speeds for the SENB tests on 2-34 (15%) and 2-34 (20%) gels, respectively. The load-displacement data shown in Fig. 9 were used to obtain the fracture toughness and Young's modulus

using methods in the ESIS protocol [5]. Due to sagging of the samples prior to loading (see Fig. 10), these curves were corrected by adding half of the specimen weight to the measured loads. This value was found by comparing the bending moment at the mid span of two beams, one with a uniformly distributed load (weight) and the other with a concentrated load at mid span.

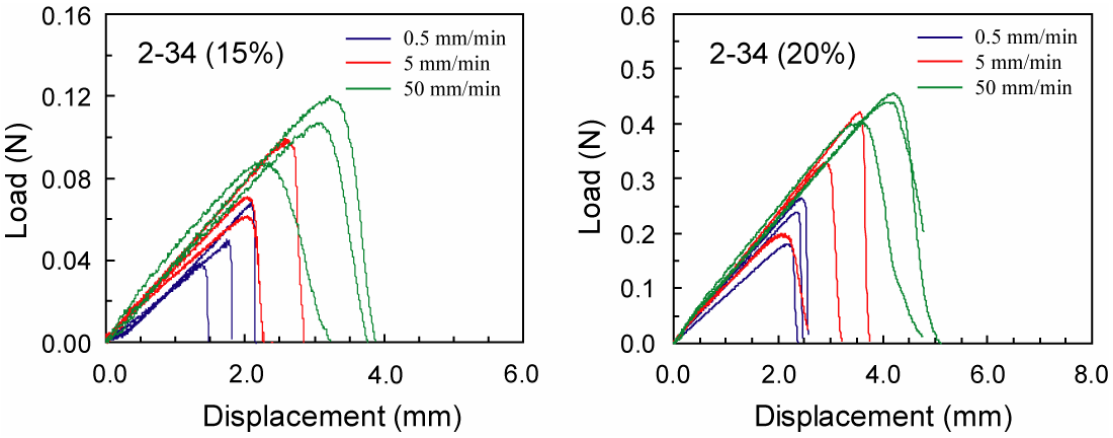

(a) (b)

FIG. 9: Experimental SENB data at different cross-head speeds for (a) 2-34 (15%) and (b) 2-34 (20%).

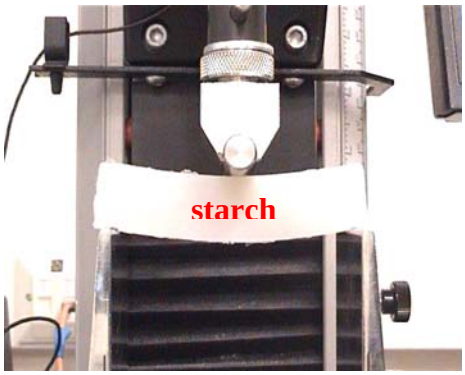

Fig. 10: Sagging of SENB sample prior to loading.

The G_c values of 2-34 (15%) and 2-34 (20%) are compared with those deduced from the wire cutting in Figs. 11(a) and 11(b), respectively. The cutting and SENB loading speeds were converted into strain rate using the FE technique described earlier. The standard deviations of the G_c from the wire cutting data were calculated using a linear regression analysis described in [7]. It is seen here that the wire cutting tests are consistently higher compared to the SENB results but the G_c values from both tests are still in the same order of magnitude. These discrepancies may be due to various reasons such as the extrapolation to zero to find G_c from the wire cutting data or the correction of sample weight in the SENB tests. In addition, the G_c values in the wire cutting are for crack propagation whereas those from the SENB tests are for crack initiation. However, both wire cutting and SENB tests agree that G_c increases with increasing rate of loading, confirming the fracture rate dependent behaviour.

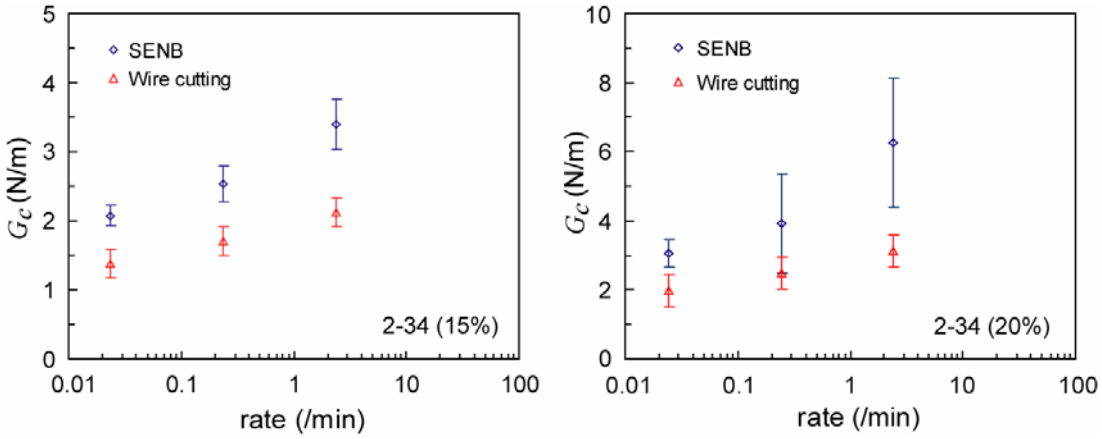

(a) (b)

FIG. 11: Predictions of fracture toughness from SENB and wire cutting tests for (a) 2-34 (15%) and (b) 2-34 (20%).

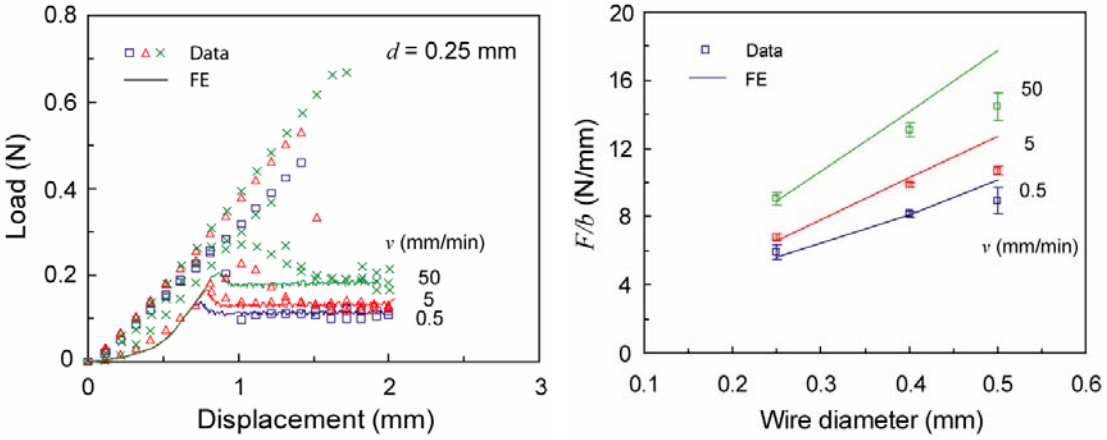

(a) (b)

FIG. 12: Comparison of steady state cutting forces (F/b) between FE simulations and experimental data for 2-34 (15%) with (a) d = 0.25 mm and (b) various wire diameters.

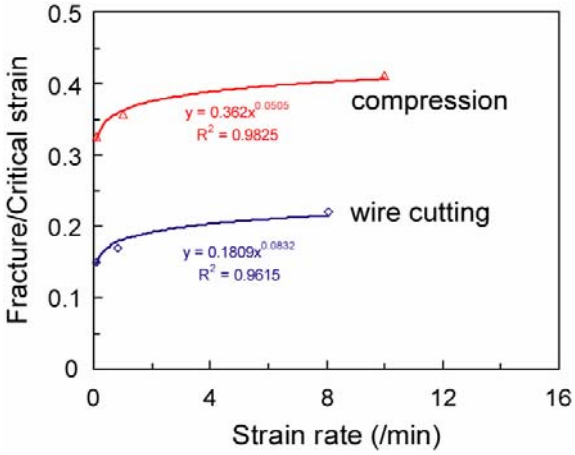

FIG. 13: Comparison of critical strain and fracture strain values of 2-34 (15%) from wire cutting simulations and compression data.

Numerically, wire cutting simulations have been performed on the 2-34 (15%) gel. By choosing appropriate values of critical strain for each cutting speed, the steady state cutting forces for d = 0.25 mm were matched with the experimental data (see Fig. 12(a)). These critical strain values were found to be 0.15, 0.17 and 0.22 for the cutting speeds of 0.5, 5 and 50 mm/min, respectively. In order to verify these critical strain values, simulations were performed on the bigger wire diameters of 0.4 and 0.5. For these diameters, the same critical strain values were used as for the 0.25 mm diameter case, whereas the critical distance l was determined from the simulations of the indentation phase. The predictions steady state values of F/b are shown in comparison with the experimental data in Fig. 12(b). Reasonable agreement between the prediction of the steady-state cutting force and the experimental data is obtained. These critical strain values are compared with the fracture strains from the compression data in Fig. 13 [4]. The results are encouraging as they follow the same trend with increasing rate. In addition, the critical strain values found from the wire cutting tests which can be assumed to represent the tensile fracture strains, are approximately one half of the compressive fracture strains. These results should be further investigated and could be verified by performing uniaxial tension experiments.

5 CONCLUSION

The values of fracture toughness from wire cutting were found to be relatively small and increased with deformation rate. The results were in reasonable agreement with those obtained from SENB tests, confirming the reliability of the cutting experiment. The numerical simulation of wire cutting process, assuming a critical strain as the failure criterion, were successful in predicting the steady state cutting forces at various cutting speeds and wire diameters.

6 ACKNOWLEDGEMENTS

Support of this work has been provided ICI under the SRF scheme. ABAQUS was provided under academic license by HKS Inc., Providence, Rhode Island, USA.

REFERENCE

[1] S.M. Goh, M. Charalambides and J.G. Williams, On the mechanics of wire cutting of cheese, Eng Fract Mech 72 (2005) 931-946.
[2] I. Kamyab, S. Chakrabarti and J.G. Williams, Cutting cheese with wire, J Mater Sci 33 (1998) 2763-2770.
[3] H. Luyten and T. Van Vliet, Fracture properties of starch gels and their rate dependency, J Texture Stud 26 (1995) 281-298.
[4] C. Gamonpilas, M. Charalambides, J.G. Williams, P.J Dooling and S. R. Gibbon, Characterisation of large deformation behaviour of starch gels using compression and indentation techniques, Proc. Int. Cong. Rheol. XVth (2008) 1189-1191.
[5] J.G. Williams and M.J. Cawood, A linear elastic fracture mechanics (LEFM) standard for determining K_c and G_c for plastics, Polym Testing 9 (1990) 15.
[6] ABAQUS Version 6.4, Hibbitt Karlsson and Sorensen Inc, Providence, RI., 2004

[7] J.G. Williams and M. Rink, The standardisation of the EWF test, Eng Fract Mech 74 (2007) 1009-1017.